

# Effect of Physicochemical Anomalies of Soda-Lime Silicate Slides on Biomolecule Immobilization

Stella H. North,<sup>†</sup> Evgeniya H. Lock,<sup>‡</sup> Tiffany R. King,<sup>†</sup> James B. Franek,<sup>‡,§</sup> Scott G. Walton,<sup>‡</sup> and Chris R. Taitt<sup>\*,†</sup>

Center for Bio/Molecular Science & Engineering and Plasma Physics Division, U.S. Naval Research Laboratory, 4555 Overlook Ave. SW, Washington, D.C. 20375

Glass microscope slides are considered by many as the substrate of choice for microarray manufacturing due to their amenability to various surface chemistry modifications. The use of silanes to attach various functional groups onto glass slides has provided a versatile tool for the covalent immobilization of many diverse biomolecules of interest. We recently noted a dramatic reduction in biomolecule immobilization efficiency on standard microscope slides prepared using a well-characterized silanization method. A survey of commercial soda-lime slides yielded the surprising result that slides purchased prior to 2008 had superior immobilization efficiencies when compared to those purchased after 2008. Characterization of the slides by X-ray photoelectron spectroscopy (XPS), contact angle measurements, and atomic force microscopy (AFM), revealed a significant correlation ( $R > 0.9$ ) between magnesium content, surface roughness, and bioimmobilization efficiency. High performance slides had higher magnesium content and higher root-mean-square (rms) roughness ( $P < 0.005$ ) than slides with lower bioimmobilization efficiencies. Although the exact mechanism of how magnesium content and surface roughness affect silane deposition has not yet been defined, we show that recent changes in the chemical and physical properties of commercial soda-lime slides affect the ability of these slides to be covalently modified.

Glass microscope slides are considered by many to be the substrate of choice for microarray manufacturing due to their low cost, stability at high temperatures, broad availability, non-porosity, low intrinsic fluorescence, and amenability to various chemical surface modifications. The wide variety of surface modifications that is commercially available on glass microscope slides underscores the importance of slide surface chemistry to the advancement of microarray technology.<sup>1–4</sup> These methods include poly-L-lysine coating,<sup>5</sup> formation of self-assembled monolayers after gold-coating,<sup>6</sup> addition of three-dimensional matrices such as polymers,<sup>7</sup> agarose,<sup>8</sup> and acrylamide-based hydrogels,<sup>9–13</sup> hydro-

phobin coating,<sup>14</sup> and silanization.<sup>3,15–20</sup> In particular, the use of silanes to attach various functionalities and reactive groups onto glass slides has provided a simple and versatile tool for the direct, covalent immobilization of different biomolecules such as oligonucleotides, cDNA, proteins, antibodies, and other molecules of interest,<sup>21,22</sup> as well as for attachment of scaffolds (e.g., dextrans) used in subsequent coupling reactions.<sup>23,24</sup> The quality of the silane coating is critical for determining uniformity and coupling efficiency of the attached molecules and often determines the overall success of the microarray experiment. Although high

\* Corresponding author. Phone: 202-404-4208. Fax: 202-404-8688. E-mail: chris.taitt@nrl.navy.mil.

<sup>†</sup> Center for Bio/Molecular Science & Engineering.

<sup>‡</sup> Plasma Physics Division.

<sup>§</sup> Global Strategies Group (North America), Inc., Crofton, MD 21114.

(1) Angenendt, P.; Glöckler, J.; Murphy, D.; Cahill, D. J. *J. Chromatogr. A* **2003**, *1009*, 97–104.

(2) Angenendt, P.; Glöckler, J.; Murphy, D.; Cahill, D. J. *Anal. Biochem.* **2002**, *309*, 253–260.

(3) Kusnezow, W.; Hoheisel, J. D. *J. Mol. Recognit.* **2003**, *16*, 165–176.

(4) Schena, M., Ed. *Protein Microarrays*; Jones and Bartlett Publishers: Sudbury, MA, USA, 2005.

(5) DiRisi-Laboratory In *DNA Microarrays: a molecular cloning manual*; Bowtell, D., Sambrook, J., Eds.; Cold Spring Harbor Laboratory Press: New York, 2003, pp 68–70.

(6) Houseman, B. T.; Huh, J. H.; Kron, S. J.; Mrksich, M. *Nat. Biotechnol.* **2002**, *20*, 270–274.

(7) Piehler, J.; Brecht, A.; Valiokas, R.; Liedberg, B.; Gauglitz, G. *Biosens. Bioelectron.* **2000**, *15*, 473–481.

(8) Afanassiev, V.; Hanemann, V.; Wolf, S. *Nucleic Acids Res.* **2000**, *28*, e66.

(9) Charles, P. T.; Goldman, E. R.; Rangasamy, J. G.; Schauer, C. L.; Chen, M. S.; Taitt, C. R. *Biosens. Bioelectron.* **2004**, *20*, 753–764.

(10) Charles, P. T.; Velez, F.; Soto, C. M.; Goldman, E. R.; Martin, B. D.; Ray, R. I.; Taitt, C. R. *Anal. Chim. Acta* **2006**, *578*, 2–10.

(11) Arenkov, P.; Kukhtin, A.; Gemmell, A.; Voloshchuk, S.; Chupeeva, V.; Mirzabekov, A. *Anal. Biochem.* **2000**, *278*, 123–131.

(12) Guschin, D.; Mobarry, B.; Proudnikov, D.; Stahl, D.; Rittmann, B.; Mirzabekov, A. *Appl. Environ. Microbiol.* **1997**, *63*, 2397–2402.

(13) Vasiliskov, A. V.; Timofeev, E. N.; Surzhikov, S. A.; Drobyshev, A. L.; Shick, V. V.; Mirzabekov, A. D. *Biotechniques* **1999**, *27*, 596–598.

(14) Qin, M.; Hou, S.; Wang, L.; Feng, X.; Wang, R.; Yang, Y.; Wang, C.; Yu, L.; Shao, B.; Qiao, M. *Colloid Surf. B* **2007**, *60*, 243–249.

(15) Letarte, M.; Voulgaraki, D.; Hatherley, D.; Foster-Cuevas, M.; Saunders, N. J.; Barclay, A. N. *BMC Biochem.* **2005**, *6*, 2.

(16) Fang, Y.; Frutos, A. G.; Lahiri, J. J. *Am. Chem. Soc.* **2002**, *124*, 2394–2395.

(17) MacBeath, G.; Koehler, A. N.; Schreiber, S. L. *J. Am. Chem. Soc.* **1999**, *121*, 7967–7968.

(18) Bhatia, S. K.; Shriver-Lake, L. C.; Prior, K. J.; Georger, J. H.; Calvert, J. M.; Bredehorst, R.; Ligler, F. S. *Anal. Biochem.* **1989**, *178*, 408–413.

(19) Shriver-Lake, L. C.; Charles, P. T.; Taitt, C. R. *Methods Mol. Biol.* **2008**, *504*, 419–440.

(20) Sapsford, K. E.; Ligler, F. S. *Biosens. Bioelectron.* **2003**, *19*, 1045–1055.

(21) Taylor, R. F.; Schultz, J. S. *Handbook of Chemical and Biological Sensors*; IOP Publishing Ltd.: London, 1996.

(22) Swalen, J. D.; Allara, D. L.; Andrade, J. D.; Chandross, E. A.; Garoff, S.; Israelachvili, J.; McCarthy, T. J.; Murray, R.; Pease, R. F.; et al. *Langmuir* **2002**, *3*, 932–950.

(23) Le Berre, V.; Trevisiol, E.; Dagkessamanskaia, A.; Sokol, S.; Caminade, A.-M.; Majoral, J. P.; Meunier, B.; Francois, J. *Nucleic Acids Res.* **2003**, *31*, e88.

(24) Lofas, S.; Johnsson, B.; Tegendahl, K.; Ronnberg, I. J. *Colloid Interface Sci.* **1993**, *65*, 423–431.

Report Documentation Page				Form Approved OMB No. 0704-0188	
Public reporting burden for the collection of information is estimated to average 1 hour per response, including the time for reviewing instructions, searching existing data sources, gathering and maintaining the data needed, and completing and reviewing the collection of information. Send comments regarding this burden estimate or any other aspect of this collection of information, including suggestions for reducing this burden, to Washington Headquarters Services, Directorate for Information Operations and Reports, 1215 Jefferson Davis Highway, Suite 1204, Arlington VA 22202-4302. Respondents should be aware that notwithstanding any other provision of law, no person shall be subject to a penalty for failing to comply with a collection of information if it does not display a currently valid OMB control number.					
1. REPORT DATE <b>2009</b>		2. REPORT TYPE		3. DATES COVERED <b>00-00-2009 to 00-00-2009</b>	
4. TITLE AND SUBTITLE <b>Effect of Physicochemical Anomalies of Soda-Lime Silicate Slides on Biomolecule Immobilization</b>				5a. CONTRACT NUMBER	
				5b. GRANT NUMBER	
				5c. PROGRAM ELEMENT NUMBER	
6. AUTHOR(S)				5d. PROJECT NUMBER	
				5e. TASK NUMBER	
				5f. WORK UNIT NUMBER	
7. PERFORMING ORGANIZATION NAME(S) AND ADDRESS(ES) <b>Center for Bio/Molecular Science &amp; Engineering and Plasma Physics Division,U.S. Naval Research Laboratory,4555 Overlook Ave. SW,Washington,DC,20375</b>				8. PERFORMING ORGANIZATION REPORT NUMBER	
9. SPONSORING/MONITORING AGENCY NAME(S) AND ADDRESS(ES)				10. SPONSOR/MONITOR'S ACRONYM(S)	
				11. SPONSOR/MONITOR'S REPORT NUMBER(S)	
12. DISTRIBUTION/AVAILABILITY STATEMENT <b>Approved for public release; distribution unlimited</b>					
13. SUPPLEMENTARY NOTES					
14. ABSTRACT					
15. SUBJECT TERMS					
16. SECURITY CLASSIFICATION OF:			17. LIMITATION OF ABSTRACT <b>Same as Report (SAR)</b>	18. NUMBER OF PAGES <b>7</b>	19a. NAME OF RESPONSIBLE PERSON
a. REPORT <b>unclassified</b>	b. ABSTRACT <b>unclassified</b>	c. THIS PAGE <b>unclassified</b>			

**Table 1. Summary of Commercially Available Soda-Lime Slides Investigated<sup>a</sup>**

slide code	name	vendor	cat. #	lot #	purchase date
A1	Daigger microslides, plain, precleaned	Daigger	G15975B		<2008
B1	Fisherfinest premium microslides, plain	Fisher Scientific	12-544-1	1690H	<2008
C1	Fisherbrand plain microscope slides	Fisher Scientific	12-550A		<2008
D1	VWR micro slides selected, precleaned, plain	VWR International	48300-025		<2008
A2	Daigger plain microslides, precleaned	Daigger	EF15975A		>2008
B2	Fisherfinest premium microslides, plain	Fisher Scientific	12-544-1	1899	>2008
C2	Fisherbrand plain microscope slides	Fisher Scientific	12-550-A3		>2008
D2	precleaned gold seal microslides, plain	Becton-Dickinson	3010		>2008

<sup>a</sup> Additional slides with limited analyses (bioimmobilization, water contact angle, and elemental composition) are described in Table S-3 in the Supporting Information.

quality slides precoated with an appropriate silane are commercially available, many microarray researchers custom build their own arrays using well-defined protocols and inexpensive borosilicate or soda-lime slides.<sup>2,25,26</sup>

We have utilized a silane-based attachment chemistry to create arrays of immobilized biomolecules on glass slides for over 10 years.<sup>18-20,27</sup> We recently noticed, however, a dramatic reduction in immobilization efficiency when attaching both proteins and peptides to standard soda-lime microscope slides using this well-characterized method. After exhaustive evaluation of reagents, buffers, solvents, and other materials used in this work, it was determined that it was the glass slides that were solely responsible for poor immobilization efficiency. Interestingly, it was slides purchased after 2008 that had poor binding efficiency. Therefore, we sought to determine the source of this disparity between slides purchased before and after 2008 through a chemical and physical survey of commercially available soda-lime slides, assessing efficacy of biomolecule immobilization, silane deposition, chemical composition, and surface characteristics such as contact angles and roughness.

## EXPERIMENTAL SECTION

**Materials.** Standard soda-lime glass microscope slides were obtained from several sources (Table 1). Rabbit anti-lipid A (*Escherichia coli*) IgG was purchased from AbD Serotec (Raleigh, NC). (3-Mercaptopropyl)triethoxysilane (MTS), 4-maleimidobutyric acid *N*-hydroxysuccinimide ester (GMBS), phosphate buffered saline (PBS), pH 7.4, potassium hydroxide, Tween-20, bovine serum albumin (BSA), dimethyl sulfoxide (DMSO), and methanol were purchased from Sigma-Aldrich (St. Louis, MO).

**Cy3 Labeling of Purified Antibody (Model Protein).** Rabbit anti-lipid A was conjugated with Cy3 monoreactive dye (Amersham-Pharmacia, Piscataway, NJ) following the manufacturer's instructions. Cy3-conjugated antibodies were purified from unincorporated dye by gel filtration on BioGel P-10 (BioRad, Hercules, CA). Protein concentrations were determined according to the manufacturer's instructions.

**Cleaning and Preparation of Glass Substrate.** Slides were first rinsed with distilled water while gently rubbing the surface with gloved fingers to remove loosely bound contaminants. After

drying, slides were immersed in a solution of 10% KOH in methanol and incubated static for 2 h. Slides were then removed from the methanolic KOH solution and rinsed exhaustively with distilled water until no schlieren lines were observed. Slides were then dried, stored at room temperature, and used within 3 days. Additional methods for cleaning of slides were assessed and are described in Table S-1 in the Supporting Information.

### Silanization and Attachment of Fluorescent Biomolecule.

Slides were patterned with varying concentrations of Cy3-labeled IgG essentially as previously described.<sup>28</sup> In this work, two separate solutions were used in the silanization step, toluene and methanol. Specifically, cleaned slides were placed within a Coplin jar and covered with a solution of 2% mercaptopropyl triethoxy silane in toluene. After a 30 min incubation under nitrogen, slides were removed, rinsed three times in separate beakers of toluene, and dried. Alternatively, a 2% silane solution was prepared in methanol adjusted to pH 4 by addition of several drops of acetic acid. The silanized slides were rinsed three times in methanol before drying. Cross-linking was accomplished by placing the dried, silanized slides into a Coplin jar containing 1.0 mM GMBS in absolute ethanol and incubating for 30 min. Slides were then rinsed thrice with deionized water and dried.

Slides were then placed in contact with poly(dimethylsiloxane) patterning templates molded to contain multiple channels.<sup>29,30</sup> Dilutions of Cy3-labeled antibody (10 ng/mL to 10  $\mu$ g/mL in PBS) were injected into each lane and allowed to incubate overnight at 4 °C; each concentration was patterned in duplicate. Each channel was then rinsed with 1 mL of PBS containing 0.05% Tween-20 and 0.1% BSA (PBSTB), and the slides were removed from the patterning template. After a brief rinse under distilled water, the slides were dried and fluorescence was determined using a ScanArray Express HT laser scanner (Perkin-Elmer, Waltham, MA). Quantitative microarray analysis software was used for data extraction and fluorescence intensity analysis. Mean fluorescence values were determined from at least five different locations spanning the length of each stripe (two stripes per slide) of immobilized Cy3-antibody on duplicate slides.

**Contact Angle Measurements.** Goniometry was performed using a static sessile drop technique on the different slide sets at several points in the processing procedure: after an initial water rinse to remove attached particulates, after cleaning with KOH/

(25) Grainger, D. W.; Greef, C. H.; Gong, P.; Lochhead, M. J. In *Microarrays: Volume 1: Synthesis Methods*; Rampal, J. B., Ed.; Humana Press: NJ, 2007; Vol. 381, pp 37-57.

(26) Seong, S.-Y. *Clin. Diagn. Lab Immunol.* **2002**, *9*, 927-930.

(27) Shriver-Lake, L. C. In *Immobilized Biomolecules in Analysis*; Cass, T., Ligler, F. S., Eds.; Oxford University Press: New York, 1998, pp 1-14.

(28) Ngundi, M. M.; Taitt, C. R. *Methods Mol. Biol.* **2006**, *345*, 53-68.

(29) Feldstein, M. J.; Golden, J. P.; Rowe, C. A.; MacCraith, B. D.; Ligler, F. S. *J. Biomed. Microdevices* **1999**, *1*, 139-153.

(30) Taitt, C. R.; Shubin, Y. S.; Angel, R.; Ligler, F. S. *Appl. Environ. Microbiol.* **2004**, *70*, 152-158.

methanol (and other methods), and after silane treatment (but before cross-linking). Contact angle measurements were performed at room temperature using a goniometer (AST Products, Inc.), equipped with a microsyringe to control volume of the liquid drop (2  $\mu$ L). Four water drops were placed at different locations on each substrate surface. Eight contact angle measurements (each side of one water drop) were averaged, and the corresponding standard deviations were calculated for each slide set.

**X-ray Photoelectron Spectroscopy.** Surface elemental and chemical state analyses were performed on a K-Alpha X-ray photoelectron spectrometer (Thermo Scientific). This instrument is equipped with a microfocusing monochromator (Al K $\alpha$  X-ray source, 1486.6 eV), which was operated at a spot size of 400  $\mu$ m. Analyzer pass energies of 200 and 25 eV, respectively, were used for elemental survey and chemically sensitive narrow scan spectra. K-Alpha's charge compensation system was used during the analysis, utilizing very low energy electrons and argon ions to prevent any localized charge buildup. Spectra were referenced to the main C 1s peak at 284.8 eV and quantified using Scofield sensitivity factors.

**Atomic Force Microscopy.** Surface morphology was studied at various scales using an atomic force microscope (Nanoscope III, Veeco Metrology, Santa Barbara, CA) operated in tapping mode. Surface images were obtained from  $5 \times 5 \mu\text{m}^2$  scans using resolution of  $256 \times 256$  pixels and a scan rate of 1.5 Hz. The z-scale for as-received and KOH-treated glass was 10 nm, whereas the scale for silanized glass was 50 nm. For a quantitative evaluation of the topography changes, root-mean square (rms) roughness was calculated from the surface height data  $z_i$  using

$$R_q = \left[ \frac{1}{N} \sum_{i=1}^N |z_i - \bar{z}|^2 \right]^{1/2}$$

where  $\bar{z}$  is the mean height.

## RESULTS AND DISCUSSION

### Slide Survey–Biomolecule Immobilization Efficiencies.

The initial objective of this study was to identify commercially available, inexpensive soda-lime slides that exhibit high protein immobilization efficiency. Eight different lots of soda-lime slides, purchased at different times (prior to 2008 or after 2008), were compared. To evaluate lot-dependent slide properties, three matched sets of slides were investigated: A1, B1, and C1 (purchased before 2008) and A2, B2, and C2 (purchased after 2008) (Table 1); although catalog numbers had changed, confirmation was obtained from the manufacturers that slides in set A1 were the same soda-lime glass slides as those in set A2 and likewise with sets B1/B2 and C1/C2. Additional slides D1 (VWR; purchased before 2008) and D2 (Becton-Dickinson; purchased after 2008) were also tested. After cleaning, silanization, and cross-linker treatment, protein immobilization efficiency was determined for each slide set through fluorescence measurements of attached Cy3-labeled antibody. Figure 1A (inset, upper right) shows representative fluorescence images taken from slides purchased before and after 2008. Dose–response curves for each slide type (Figure S-1 in the Supporting Information) were used to determine detection limits, defined as the lowest concentration tested at which fluorescent signals were at least three standard deviations

above background. Figure 1A represents the mean net fluorescence from the highest concentration of Cy3-protein tested (10  $\mu$ g/mL) on each slide set and shows that slides purchased before 2008 (sets A1–D1) demonstrated significantly higher protein immobilization than those purchased after 2008 (sets A2–D2). Detection limits for all batches of pre-2008 slides silanized in toluene were 0.1  $\mu$ g/mL, whereas those for slides purchased after 2008 were at least 5-fold higher.

The solvent in which silanization is performed plays a significant role in determining both the concentration and the quality of the silane coating on a glass surface.<sup>31–33</sup> Although toluene (used here; gray bars in Figure 1A) is a common solvent for silanization of silica-based materials,<sup>34</sup> many researchers have used acidic methanol for silane deposition.<sup>32</sup> Therefore, we repeated the survey of bioimmobilization efficiencies using a methanol-based silanization protocol (white bars in Figure 1A; Figure S-1 in the Supporting Information). In all cases, fluorescent signals from slides silanized in the methanolic solvent were significantly lower than those silanized in toluene ( $P < 0.001$ ), with a consequent 10-fold increase in detection limits (1  $\mu$ g/mL for pre-2008 slides and 10  $\mu$ g/mL for post-2008 slides); in some cases, no fluorescence signals were detected at even the highest protein concentration tested (Table S-3 in the Supporting Information). As for the toluene-processed slides, the trend for slides purchased prior to 2008 outperforming the newer slides was again observed. However, the differences appeared to be more marked in the methanol-silanized slides. Slides silanized in acidic methanol exhibited an average 13-fold difference in protein binding between pre- and post-2008 slides, whereas, the difference was only 5-fold when toluene was used. In short, toluene improved protein immobilization more on the low performance slides than on the high performance slides, thereby reducing the overall performance variance between pre- and post-2008 slides. However, even under optimal silanization conditions, protein immobilization efficiencies of the post-2008 slides were still well below that of the older slides.

To ascertain that inadequate cleaning was not responsible for this effect, we conducted a study of eight well-characterized cleaning methods on the slides prior to silanization, cross-linking, and biomolecule immobilization (Table S-1 in the Supporting Information). Although some variations were observed between cleaning protocols, the same trend of higher immobilization efficiency in pre-2008 slides was observed, independent of cleaning method (Figure S-2 in the Supporting Information). For all subsequent experiments, the optimal cleaning and silanization methods were used (cleaning in 10% KOH/methanol for 2 h, followed by silanization in toluene).

Results from the bioimmobilization study suggested that the most significant difference in protein binding efficiency was correlated to the manufacture lot and, presumably, the manufacture date of the slides. Even with careful selection of microscope slides and optimization of reaction conditions, the protein immobilization efficiencies of post-2008 slides could not be improved to those of corresponding pre-2008 slides. This raised the possibility that elemental impurities and/or compositional dispari-

(31) Chen, T. M.; Brauer, G. M. *J. Dent. Res.* **1982**, *61*, 1439–1443.

(32) Hermanson, G. T. *Bioconjugate Tech.*; Academic Press: Oxford, 2008.

(33) McGovern, M. E.; Kallury, K. M. R.; Thompson, M. *Langmuir* **2002**, *10*, 3607–3614.

(34) Welch, K. J.; Hoffman, N. E. *J. High Res. Chromatogr.* **1986**, *9*, 417–419.



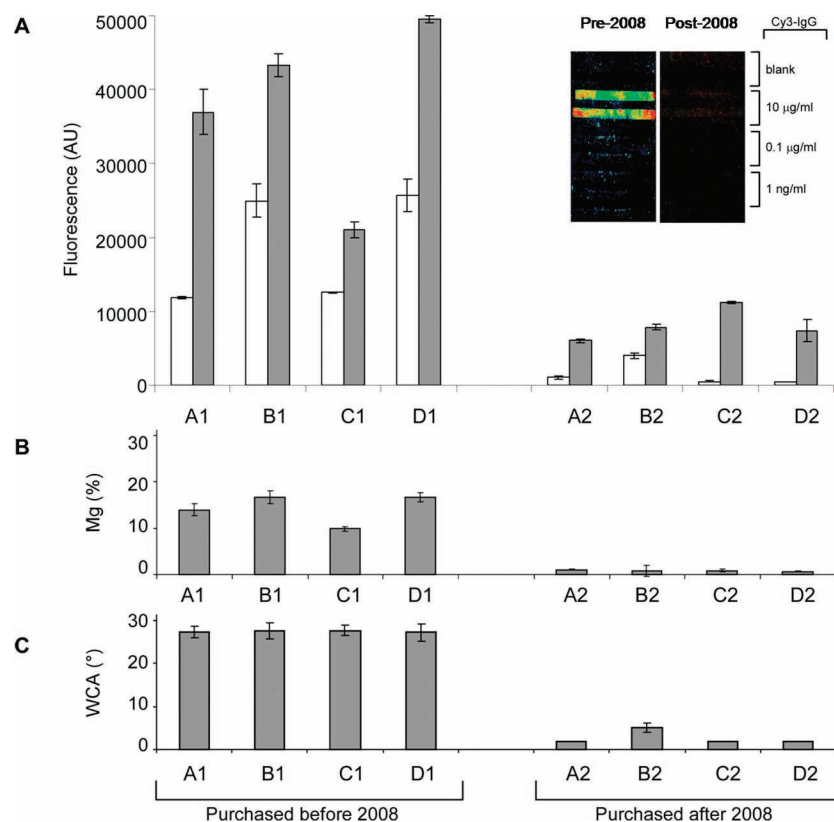


**Figure 1.** Survey of commercial soda-lime microscope slides. (A) Immobilization efficiency of Cy3-IgG (10  $\mu$ g/mL) on commercial soda-lime slides. Slides A1 through D1 were purchased prior to 2008 and slides A2 through D2 were purchased after 2008. The average fluorescence intensity and the standard deviation were determined from five different locations spanning each stripe on two replicates of each protein concentration tested on two duplicate slides. Although absolute values of fluorescence varied between sets of slides, the trend of higher immobilization on older slides was representative of all concentrations. White bars: silanization in acidic methanol; gray bars: silanization in toluene. Inset, image of representative Cy3-IgG patterned slides B1 (left) and B2 (right). Lower limit of detection for slides silanized in acidic methanol: pre-2008 = 1  $\mu$ g/mL, post-2008 = 10  $\mu$ g/mL; slides silanized in toluene: pre-2008 = 0.1  $\mu$ g/mL, post-2008 = 1  $\mu$ g/mL. (B) Atomic concentration (%) of magnesium and (C) water contact angle measurement of pre- and post-2008 slides after KOH cleaning.

ties are associated with a recent change in the manufacture of soda-lime glass slides.

**X-ray Photoelectron Spectroscopy (XPS).** To identify elemental disparities in the glass surface, relative atomic surface compositions of pre- and post-2008 soda-lime slides were determined by XPS (Table 2); XPS was also used to determine the efficiency of silanization, as the sulfur in the thiol silane provided a unique XPS-identifiable element. All slides exhibited the major elements of glass, carbon, silicon, and oxygen, as well as trace amounts of sodium, nitrogen, and calcium. Furthermore, both pre- and post-2008 slides exhibited an increase in both sulfur and carbon content after silane treatment (attributed to the addition of the silane layer), with a corresponding drop in contributions from other components as the original glass substrate became shielded with silane deposition. High resolution XPS analyses confirmed that the sulfur on the glass surfaces was present as the reactive thiol form (SH). However, slides purchased prior to 2008 revealed significantly higher concentrations of magnesium compared to the corresponding slides purchased after 2008 (Figure 1B and Table 2;  $P < 0.001$ ). The older slides also exhibited higher degrees of silanization than newer slides based on sulfur and carbon composition ( $P < 0.05$ ), and a significant, positive correlation between magnesium content and silanization efficiency was observed ( $R = 0.780$ ;  $P < 0.05$ ). Moreover, the high magnesium content was strongly related to biomolecule im-

mobilization, as calculated based on detection limits of immobilized IgG ( $R = 0.942$ ;  $P < 0.001$ ); results from four additional lots of soda-lime slides purchased at different times showed the same correlation (Table S-3 in the Supporting Information;  $R = 0.9$ ,  $P < 0.001$ ). These results suggest that a high concentration of magnesium in soda-lime glass is linked to higher silane coverage density on the slide surface, thereby affecting subsequent protein binding.

**Contact Angles.** To determine if the disparity in Mg content was correlated with other differences in surface properties (e.g., surface hydrophilicity) of the soda-lime slides, goniometry was used to qualitatively assess surface wettability of KOH-cleaned slides (Figure 1C; Table S-3 in Supporting Information). Low magnesium slides (sets A2–D2), displayed low contact angles ( $WCA < 5^\circ$ ), with most exhibiting total wetting, recorded as  $WCA \approx 2^\circ$ . In contrast, high magnesium slides (sets A1–D1) displayed a mean contact angle of  $27.49 \pm 0.10^\circ$ . It should be noted that the mean contact angle values for “as-received” slides (no treatment) were only slightly higher than KOH-cleaned slides ( $\approx 5.0^\circ$ ), indicating that the considerable difference in contact angle values between the pre- and post-2008 slides was not due to KOH treatment. The results suggest compositional and structural differences at the surfaces, either of which can be attributed to surface contaminants or alkali leaching. XPS analyses performed after additional cleaning treatments designed to remove heavy

**Table 2. Relative Atomic Concentrations and Standard Deviations<sup>a</sup> of the Measured Elements<sup>b</sup> (C, Si, O, Mg, S) on KOH-Cleaned (KOH) and Mercaptosilane-Treated (Si) Soda-Lime Slides<sup>c</sup>**

slide/treatment	C (%)	Si (%)	O (%)	Mg (%)	S (%)	p-value <sup>d</sup>	LOD ( $\mu\text{g/mL}$ )
A1/KOH	13.60 $\pm$ 0.40	19.91 $\pm$ 0.80	48.91 $\pm$ 1.20	13.87 $\pm$ 1.29	ND <sup>e</sup>		
A2/KOH	12.98 $\pm$ 0.09	26.94 $\pm$ 0.15	56.47 $\pm$ 0.31	1.06 $\pm$ 0.04	ND		
A1/Si	23.36 $\pm$ 2.34	20.69 $\pm$ 0.91	44.98 $\pm$ 2.25	5.33 $\pm$ 2.04	2.40 $\pm$ 0.39		0.1
A2/Si	15.45 $\pm$ 5.19	27.21 $\pm$ 0.89	52.57 $\pm$ 2.03	0.21 $\pm$ 0.25	1.63 $\pm$ 0.61	$p < 0.05$	1.0
B1/KOH	13.86 $\pm$ 0.71	19.21 $\pm$ 0.88	48.55 $\pm$ 0.69	16.67 $\pm$ 1.44	ND		
B2/KOH	14.95 $\pm$ 0.83	25.68 $\pm$ 0.29	54.28 $\pm$ 3.16	0.81 $\pm$ 1.14	ND		
B1/Si	24.42 $\pm$ 3.45	20.99 $\pm$ 0.30	44.96 $\pm$ 0.69	5.55 $\pm$ 1.14	2.95 $\pm$ 0.55		0.1
B2/Si	18.68 $\pm$ 1.04	25.84 $\pm$ 1.55	49.40 $\pm$ 3.16	0.28 $\pm$ 0.11	2.14 $\pm$ 0.13	$p < 0.05$	1.0
C1/KOH	15.81 $\pm$ 0.04	22.25 $\pm$ 0.12	50.66 $\pm$ 2.01	9.84 $\pm$ 0.49	ND		
C2/KOH	13.14 $\pm$ 0.36	26.67 $\pm$ 0.52	56.57 $\pm$ 0.43	0.86 $\pm$ 0.25	ND		
C1/Si	20.80 $\pm$ 1.05	23.01 $\pm$ 1.11	46.71 $\pm$ 1.91	5.44 $\pm$ 0.72	2.17 $\pm$ 0.11		0.1
C2/Si	16.36 $\pm$ 3.45	27.11 $\pm$ 0.19	51.65 $\pm$ 0.26	1.65 $\pm$ 0.19	1.94 $\pm$ 0.15	$p < 0.05$	1.0
D1/KOH	12.99 $\pm$ 0.64	20.01 $\pm$ 0.44	50.36 $\pm$ 0.17	16.65 $\pm$ 0.93	ND		
D2/KOH	13.07 $\pm$ 0.28	26.97 $\pm$ 0.22	56.67 $\pm$ 0.95	0.69 $\pm$ 0.05	ND		
D1/Si	23.85 $\pm$ 1.81	21.11 $\pm$ 0.96	44.65 $\pm$ 0.85	6.13 $\pm$ 0.45	3.07 $\pm$ 0.42		0.1
D2/Si	17.77 $\pm$ 1.13	26.41 $\pm$ 0.72	50.30 $\pm$ 1.35	0.77 $\pm$ 0.30	2.16 $\pm$ 0.26	$p < 0.005$	1.0

<sup>a</sup> Standard deviations of four to five replicate measurements for silane-treated slides. Standard deviations of two replicate measurements for KOH-etched slides. <sup>b</sup> Calcium, sodium, and nitrogen were present in many samples and are included in Table S-2 in the Supporting Information. <sup>c</sup> Lower limit of detection (LOD) for protein immobilization corresponding to each silane-treated slide. <sup>d</sup> Comparison of carbon and sulfur atomic composition of silane-treated slides: A1 and A2, B1 and B2, C1 and C2, and D1 and D2. <sup>e</sup> Not detected.

metals from glass surfaces<sup>35</sup> confirmed that the high magnesium content of slides A1, B1, C1, and D1 was preserved and, thus, magnesium is not a surface contaminant but appears to be found throughout the bulk. In addition, XPS data show equivalent carbon concentrations across all KOH treated slides (Table 2) and, thus, no adventitious carbon due to organic contaminants is responsible for the increased contact angles.

**Atomic Force Microscopy.** An additional variable affecting contact angle is surface roughness. In general, surface roughness increases the water contact angle for a droplet on a hydrophobic surface (i.e., WCA > 90°), whereas it tends to decrease the contact angle for a droplet on a hydrophilic one (i.e., WCA < 90°),<sup>36,37</sup> a phenomenon driven primarily by capillary action of the roughened surface.<sup>38</sup> AFM was used to examine surface topography and determine the root-mean-square (rms) roughness of a representative matched slide set, slides B1 (pre-2008, high Mg) and B2 (post-2008, low Mg). Figure 2A shows the topography of as-received slide sets B1 and B2. Surprisingly, set B1 exhibited a significantly rougher surface than set B2 as evidenced by the rms roughness value of 0.63  $\pm$  0.07 nm, which is about twice the value observed for B2 slides (0.27  $\pm$  0.02 nm;  $P < 0.002$ ). Additional AFM analysis on larger areas of 10  $\times$  10  $\mu\text{m}^2$  and 20  $\times$  20  $\mu\text{m}^2$  indicated that the differences of the surface morphology are independent of scanned area and are, thus, glass specific. KOH treatment (Figure 2B) resulted in an approximate 3-fold increase in the rms roughness value of B1 slides (1.71  $\pm$  0.42 nm;  $P < 0.005$ ), which is consistent with previous reports for KOH-etching.<sup>39</sup> In contrast, B2 slides exhibited minimal change in surface roughness after

the KOH-etch (0.40  $\pm$  0.17 nm;  $P > 0.2$ ), with pre-2008 slides still exhibiting significantly greater nanoscale roughness. After silanization, the rms roughness values for both slide sets were not significantly different: 1.36  $\pm$  0.03 nm and 1.35  $\pm$  0.01 nm for B1 and B2 slides, respectively (Figure 2C;  $P > 0.5$ ). Here, however, one should consider this similarity with caution: the presence of large, isolated peaks in the post-2008 slides can skew the rms values. The images in Figure 2C clearly differ in topography and line scans taken at various locations (Figure S-3 in the Supporting Information) also indicate a difference. For the latter, it appears that if one considers only the areas between the large, isolated peaks on the surfaces of the post-2008 slides, they are smoother than the pre-2008 slides. Although the differences are difficult to quantify from only the images and select lines scans, it is reasonable to assume that over much of the scanned areas, the substrate surface roughness is preserved through the silane layer.

**Effect of Physicochemical Surface Properties of Soda-Lime Glass on Bioimmobilization.** Our experimental results show that the contact angles, surface roughness, and chemical composition of the sets of investigated slides (purchased before and after 2008) are different. Even though the complex relationship between glass surface characteristics and biomolecule immobilization is not thoroughly understood, the results suggest that a high concentration of magnesium in soda-lime glass slides is linked to higher silane coverage density on the slide surface, thereby affecting subsequent protein binding.

It is well-known that the chemical composition of glass, i.e., the presence of alkali metal oxides (e.g., Na<sub>2</sub>O, K<sub>2</sub>O) and alkaline earth oxides (e.g., MgO, CaO), affects the mechanical and dissolution properties of glass.<sup>40–43</sup> In general, the incorporation

(35) Kern, W.; Puotinen, D. A. *RCA Rev.* **1970**, *31*, 187–206.

(36) Johnson, R. E., Jr.; Dettre, R. H. In *Advances in Chemistry Series*; Gould, R. F., Ed.; American Chemical Society: Los Angeles, CA, 1964, pp. 136–144.

(37) Busscher, H. J.; van Pelt, A. W. J.; de Boer, P.; de Jong, H. P.; Arends, J. *Colloids Surf.* **1984**, *9*, 319–331.

(38) Kamusewitz, H.; Possart, W.; Paul, D. *Colloid Surf., A* **1999**, *156*, 271–279.

(39) Rädlein, E.; Frischat, G. H. J. *Non-Cryst. Solids* **1997**, *222*, 69–82.

(40) Dietrich, E.; Oudadesse, H.; Lucas-Girot, A.; Le Gal, Y.; Jeanne, S.; Cathelineau, G. *Applied Surface Science: The First International Symposium on Surfaces and Interfaces of Biomaterials* **2008**, *255*, 391–395.

(41) Dietrich, E.; Oudadesse, H.; Lucas-Girot, A.; Mami, M. J. *Biomed. Mater. Res., Part A* **2009**, *88A*, 1087–1096.

(42) Oelkers, E. H.; Schott, J. *Geochim. Cosmochim. Acta* **2001**, *65*, 1219–1231.

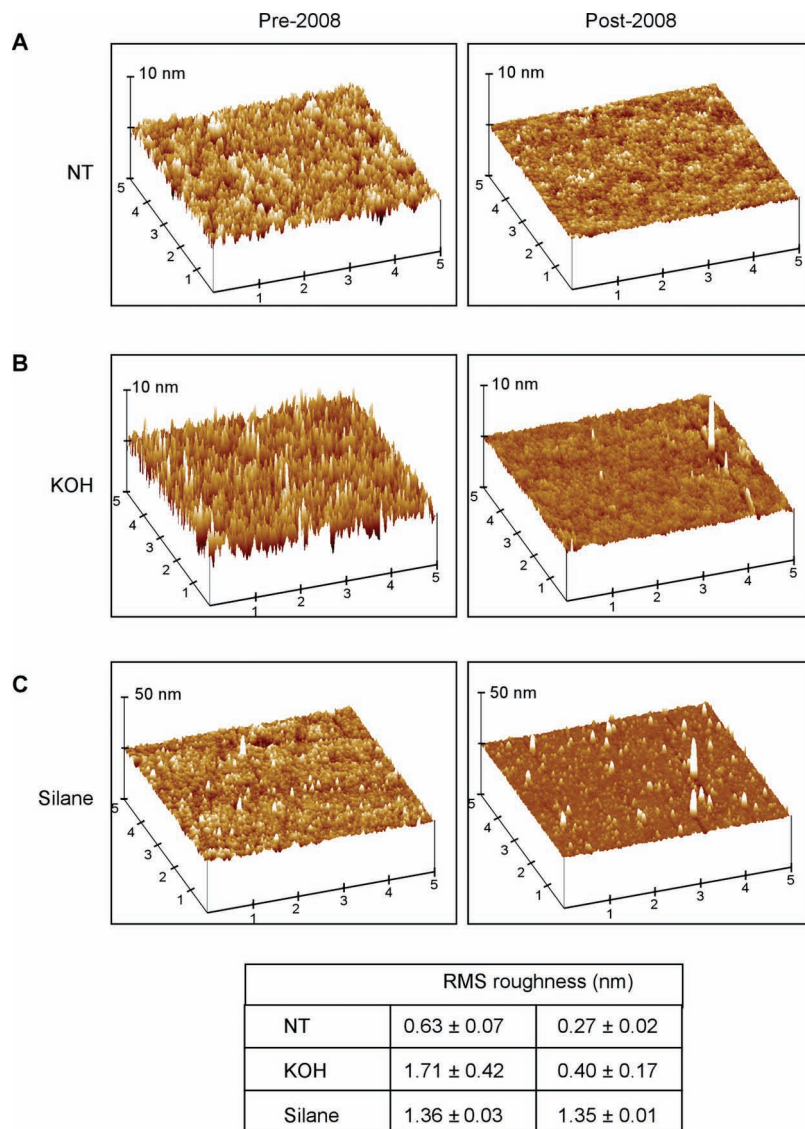


**Figure 2.** Surface roughness as a function of treatment conditions on set B1 slides (purchased before 2008) and set B2 slides (purchased after 2008). Representative AFM three-dimensional images for slides (A) “as-received” with no treatment (NT), (B) after KOH-cleaning treatment (KOH), and (C) after silanization in toluene. Averaged rms roughness values and standard deviations were calculated from three measurements at different locations on untreated, KOH-methanol cleaned, and silanized slides.

of any alkaline oxide in glass results in the modification of the three-dimensional siloxane (Si–O–Si) network. Alkali cations break siloxane bonds and form nonbridging oxygens, leading to the formation of highly reactive silanol groups ( $\equiv\text{Si}-\text{OH}$ ). But during the initial stages of glass dissolution, *alkali metal* cations (e.g., Na and K) tend to preferentially leach out of the glass. This process initiates the rearrangement of the leached layer network structure and promotes the reformation of siloxane bonds.<sup>44</sup> In contrast, *alkaline earth* cations (e.g., Mg and Ca) have demonstrated the ability to block alkali diffusion, thereby preserving the silanol groups in the leached layer, and increase glass durability.<sup>43,45</sup>

Depending on the chemical composition of the glass, the leaching stage of glass dissolution proceeds in different steps. In general, the equilibrium reaction rates for bonds broken by water

absorption decreases as follows  $\text{Na}-\text{H} > \text{Ca}-\text{H} > \text{Mg}-\text{H} > \text{Al}-\text{H} > \text{Si}-\text{O}$ .<sup>42,45</sup> According to manufacturers’ specification data, soda-lime glass is composed of (approximately) 72% silicon dioxide, 14% sodium oxide, 6% calcium oxide, 4% magnesium oxide, and <2% aluminum oxide, potassium oxide, sulfur trioxide, and iron oxide. However, the XPS elemental analysis showed that the two categories of soda-lime glasses (pre- and post-2008) had significantly different atomic concentrations of silicon, oxygen, and magnesium at the surface. (The analysis depth of XPS is ~9 nm.)

We speculate that the different dissolution properties of high- and low-Mg soda-lime slides produce distinct etch profiles comprising peaks and valleys representing regions of Mg enrichment and Na depletion, respectively.<sup>46</sup> This hypothesis is supported by the AFM measurements showing differences in the surface roughness of untreated pre- and post-2008 slides, presumably due to nonuniform leaching of the high-Mg slides in the

(43) Koenderink, G. H.; Brzesowsky, R. H.; Balkenende, A. R. *J. Non-Cryst. Solids* **2000**, 262, 80–98.

(44) Scholze, H. *Glass - Nature, Structure, and Properties*; Springer-Verlag: New York, 1991.

(45) Sinton, C. W.; LaCourse, W. C. *Mater. Res. Bull.* **2001**, 36, 2471–2479.

(46) Sharma, A.; Carnali, J. O.; Lugo, G. M.; Jain, H. *J. Non-Cryst. Solids* **2002**, 311, 93–98.

presence of atmospheric moisture (Figure 2A). As expected, the nonuniformity of the high-Mg slides become even more pronounced after KOH-etching (Figure 2B, left panel),<sup>47</sup> on the other hand, more uniform glass dissolution in low-Mg slides produce only a slight increase in roughness (Figure 2B, right panel). The correlation between surface roughness and Mg content suggests a physical explanation (i.e., increased surface area) for improved silanization efficacy on the high-Mg soda-lime slides. In addition, differences in surface reactivity due to the distinct chemical composition of the slides purchased prior to 2008 may also play a role in enhanced biomolecule immobilization.

Successful and reproducible silane monolayer assembly requires reactive silanol groups ( $\equiv\text{Si}-\text{OH}$ ), which are readily available on a clean, KOH-treated glass surface. Such a surface is typically characterized by low water contact angles ( $\text{WCA} < 10^\circ$ ). Therefore, it was unexpected that the high performance, pre-2008 slides showed higher contact angle values than the post-2008 slides. However, the surfaces are still considered hydrophilic for both pre- and post-2008 slides, and the contact angle values of the silanized surfaces were similar (mean contact angles of  $68.25 \pm 2.74^\circ$  and  $66.34 \pm 1.46^\circ$ , respectively). Although XPS confirmed that silanization had occurred on all slides, further examination of the atomic concentrations of carbon and sulfur of the silanized surfaces suggested better silanization of the pre-2008 slides. These results are consistent with bioimmobilization data that clearly showed increased protein binding efficiency on these slides. These findings also suggest that the amount and the density of surface silanol groups in the pre-2008 slides are higher. It should be noted that their concentrations and distribution were not quantified.

One possible explanation for the observed phenomenon is that for *mixed* alkali silica glass, where the magnesium in the leached layer is preserved, the condensation of silanol groups is limited and, thus, a higher concentration of surface hydroxyls is formed. As a result, the relative silane deposition of the high-Mg slides is enhanced, as compared to the low-Mg soda-lime slides. Another factor that may influence the silanization efficacy of the pre- and post-2008 slides, taking into account their inherent differences in

chemistry and morphology, is the formation of different forms of silanols (e.g., single, germinal, and vicinal) on silica that differ in interaction energy<sup>48,49</sup> and acidity.<sup>50</sup>

## CONCLUSION

This work presents a physicochemical survey of commercial soda-lime microscope slides commonly used for immobilization of biomolecules in microarrays. To our surprise, it was observed that all the lots of commercial microscope slides that were purchased before 2008 had significantly higher immobilization efficiencies than those purchased after 2008 and that these high immobilization efficiencies correlated positively with chemical composition (high magnesium content) and surface morphology (roughness). To our knowledge, this is the first time these correlations have been documented in a survey of commercial substrates. The results indicate variations in the chemical composition of commercial soda-lime slides have a profound effect on the ability to immobilize biomolecules utilizing covalent silane chemistry. We anticipate that our results will be of great interest to researchers and industries involved in the custom-preparation or commercial fabrication of soda-lime slide-based arrays using standard silane chemistry.

## ACKNOWLEDGMENT

S.H.N. and E.H.L. contributed equally to this work. The authors thank Drs. Marie Archer and Gusphyl Justin for their contribution of materials, technical assistance, and helpful discussions. S.H.N. and E.H.L. are recipients of the American Society of Engineering Education and National Research Council postdoctoral fellowships, respectively. T.R.K. was supported by an NSF Historically Black Colleges and Universities-Tribal College or University internship program. This work is funded by Joint Science & Technology Office for Chemical & Biological Defense/Defense Threat Reduction Agency and the Office of Naval Research. The views expressed here are those of the authors and do not represent the opinions of the U.S. Navy, the U.S. Department of Defense, or the U.S. government.

## SUPPORTING INFORMATION AVAILABLE

Additional information as noted in the text. This material is available free of charge via the Internet at <http://pubs.acs.org>.

Received for review October 14, 2009. Accepted November 27, 2009.

AC902324R

(47) Spierings, G. A. C. M. *J. Mater. Sci.* **1993**, *28*, 6261–6273.

(48) Rudzinski, W.; Waksmundzki, A.; Lebeda, R.; Suprynowicz, Z.; Lason, M. *J. Chromatogr., A* **1974**, *92*, 25–32.

(49) Waksmundzki, A.; Rudzinski, W.; Suprynowicz, Z.; Lebeda, R.; Lason, M. *J. Chromatogr., A* **1974**, *92*, 9–23.

(50) Méndez, A.; Bosch, E.; Rosés, M.; Neue, U. D. *J. Chromatogr., A* **2003**, *986*, 33–44.